# The exocytic Rabs Ypt3 and Ypt2 regulate the early step of biogenesis of the spore plasma membrane in fission yeast

Kazuki Imada and Taro Nakamura*
Department of Biology, Graduate School of Science, Osaka City University, Sumiyoshi-ku, Osaka 558-8585, Japan

**ABSTRACT** **During fission yeast sporulation, a membrane compartment called the forespore membrane (FSM) is newly formed on the spindle pole body (SPB). The FSM expands by membrane vesicle fusion, encapsulates the daughter nucleus resulting from meiosis, and eventually matures into the plasma membrane of the spore. Although many of the genes involved in FSM formation have been identified, its molecular mechanism is not fully understood. Here a genetic screen for sporulation-deficient mutations identified Ypt3, a Rab-family small GTPase known to function in the exocytic pathway. The *ypt3-ki8* mutant showed defects in both the initiation of FSM biogenesis and FSM expansion. We also show that a mutation in Ypt2, another Rab protein that may function in the same pathway as Ypt3, compromises the initiation of FSM formation. As meiosis proceeds, both GFP-Ypt3 and GFP-Ypt2 are observed at the SPB and then relocalize to the FSM. Their localizations at the SPB precede FSM formation and depend on the meiotic SPB component Spo13, a putative GDP/GTP exchange factor for Ypt2. Given that Spo13 is essential for initiating FSM formation, these results suggest that two exocytic Rabs, Ypt3 and Ypt2, regulate the initiation of FSM formation on the SPB in concert with Spo13.**

**Monitoring Editor**
Fred Chang
University of California, San Francisco

Received: Mar 11, 2016
Revised: Aug 29, 2016
Accepted: Sep 7, 2016

## INTRODUCTION

Sporulation in the fission yeast *Schizosaccharomyces pombe* is an intriguing cellular process that accompanies meiosis and also a cell specialization process that culminates in the formation of ascospores (Shimoda, 2004; Shimoda and Nakamura, 2004). A significant feature of sporulation is the de novo biogenesis of a double unit membrane called the forespore membrane (FSM) within the cytoplasm of the diploid mother cell (Yoo *et al.*, 1973; Hirata and Tanaka, 1982; Tanaka and Hirata, 1982; Nakamura *et al.*, 2001). The FSM expands by membrane vesicle fusion, which is followed by FSM closure, resulting in the formation of a prespore containing a haploid nucleus produced in meiosis (Hirata and Shimoda, 1994; Nakamura *et al.*, 2008). After capture of the nucleus within the prespore, formation of the spore wall proceeds via deposition of spore wall materials between inner and outer layers of the FSM (Yoo *et al.*, 1973; Hirata and Tanaka, 1982). The inner layer of the FSM becomes the plasma membrane of the nascent spore, and the outer layer eventually degrades during sporulation.

Assembly of the FSM initiates in the vicinity of the spindle pole body (SPB), which is equivalent to the centrosome of animal cells, during meiosis II. Before formation of the FSM, thick, multilayered, disk-shaped structures termed meiotic outer plaques form on the cytoplasmic side of the SPB (Hirata and Shimoda, 1994). This morphological alteration, referred to as SPB modification, is presumed to be indispensable for the initiation of FSM formation. Four SPB components essential for SPB modification have been identified—Spo2, Spo13, Spo15, and the calmodulin Cam1 (Takeda and Yamamoto, 1987; Takeda *et al.*, 1989; Ikemoto *et al.*, 2000; Nakamura *et al.*, 2008; Itadani *et al.*, 2010). During vegetative growth, the coiled-coil protein Spo15 is constitutively localized at the SPB in a Cam1-dependent manner (Itadani *et al.*, 2010). At meiosis I, Spo2 and Spo13 are expressed and recruited to the SPB, dependent on the presence of Spo15 (Nakase *et al.*, 2008). When meiosis II starts, another meiotic SPB component, Spo7, localizes to the SPB independently of Spo2, Spo13, Spo15, and Cam1 and is believed to

This article was published online ahead of print in MBoC in Press (http://www.molbiolcell.org/cgi/doi/10.1091/mbc.E16-03-0162) on September 14, 2016.

*Address correspondence to: Taro Nakamura (taronaka@sci.osaka-cu.ac.jp).

Abbreviations used: FSM, forespore membrane; GEF, guanine nucleotide exchange factor; SPB, spindle pole body.

© 2016 Imada and Nakamura. This article is distributed by The American Society for Cell Biology under license from the author(s). Two months after publication it is available to the public under an Attribution–Noncommercial–Share Alike 3.0 Unported Creative Commons License (http://creativecommons.org/licenses/by-nc-sa/3.0).

"ASCB®," "The American Society for Cell Biology®," and "Molecular Biology of the Cell®" are registered trademarks of The American Society for Cell Biology.

coordinate formation of the leading edge of the FSM and the initiation of FSM assembly, thereby accomplishing accurate formation of this membrane (Nakamura-Kubo *et al.*, 2011). An intriguing unresolved aspect of the initiation of FSM formation concerns which component of the SPB serves as the nucleation site for new membranes. Spo2, Spo13, Spo15, and Cam1 do not have domains associated with lipid-binding ability (Nakase *et al.*, 2008), whereas Spo7 has a pleckstrin homology domain that can bind phospholipids within biological membranes. However, this domain is not essential for the initiation of FSM assembly (Nakamura-Kubo *et al.*, 2011). Therefore unknown SPB components that anchor the FSM may be involved in meiosis-specific functions.

To ensure an orderly flow of membrane–vesicle traffic, vesicles must be highly selective in recognizing the appropriate target membrane with which to fuse. Ras-like guanine nucleotide-binding proteins, termed Ypts in yeast or Rabs in mammals, are highly conserved throughout evolution and play a central role in this process (Segev, 2001; Stenmark and Olkkonen, 2001; Takai *et al.*, 2001). Each Rab protein has a characteristic distribution on cell membranes, and every organelle has at least one Rab protein on its cytosolic surface. Each Rab is essentially activated by a specific guanine nucleotide exchange factor (GEF), leading to its localization at a specific membrane (Blümer *et al.*, 2013; Cabrera and Ungermann, 2013). Active GTP-bound Rab associates with the membrane via its geranylgeranylated C-terminus and recruits its effectors to the membrane, where they mediate various processes of vesicle transport (Pfeffer, 2001; Stenmark and Olkkonen, 2001). A regulatory mechanism termed the Rab cascade is involved in *Saccharomyces cerevisiae* exocytosis. In this cascade, the first Rab (ScYpt32) recruits the exchange factor (ScSec2) for its downstream Rab (ScSec4) to Golgi-derived secretory vesicles (Ortiz *et al.*, 2002; Grosshans *et al.*, 2006b; Medkova *et al.*, 2006). The Rab cascade seems to be a general pathway conserved throughout evolution because similar cascades have been reported both in mammalian cells and at additional stages of membrane trafficking (Stenmark, 2009; Das and Guo, 2011; Hutagalung and Novick, 2011; Suda and Nakano, 2012; Pfeffer, 2013).

Components of the Rab cascade (Ypt3, Sec2, and Ypt2) are also highly conserved in *S. pombe*, and a mutation in either *ypt3*$^+$ or *ypt2*$^+$ severely inhibits post-Golgi membrane trafficking (Haubruck *et al.*, 1990; Craighead *et al.*, 1993; Cheng *et al.*, 2002). Of interest, Spo13 shares homology with the GEF domain of ScSec2 and can function as a GEF for Ypt2 (Yang and Neiman, 2010), implying that Ypt2 might be involved in the initiation of FSM formation. In this study, we investigated the role of these Rab proteins in *S. pombe* sporulation and discuss how, as meiotic SPB components, they regulate the initiation of FSM formation on the SPB.

## RESULTS

### Ypt3 is required for the initiation of FSM formation and expansion of the FSM

Although studies of sporulation-deficient mutants (*spo* mutants) have led to the identification of many genes involved in sporulation, the molecular mechanism underlying sporulation is not completely understood. To gain further insight into the sporulation process, we isolated a novel *spo* mutant named *spo26-ki8* (Figure 1A) from mutagenized *Schizosaccharomyces pombe* cells in which the FSM was visualized by green fluorescent protein (GFP)–tagged Psy1, an FSM-resident protein (Nakamura *et al.*, 2001). The isolation and characterization of other *spo* mutants will be discussed elsewhere. The *spo26* mutant also exhibited temperature-sensitive vegetative growth (Figure 1B), indicating that the *spo26*$^+$ gene is required not only for sporulation, but also for vegetative growth. The *spo26*$^+$

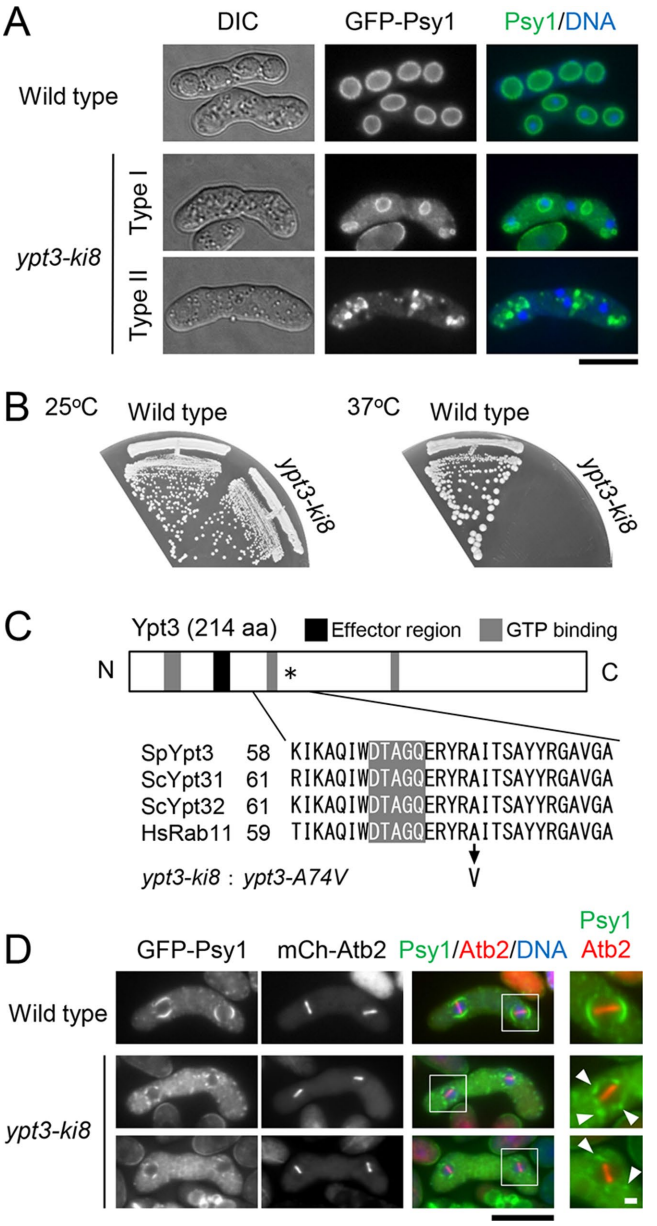


FIGURE 1: The *ypt3-ki8* mutant shows defects in both initiation of FSM formation and expansion of the FSM. (A) FSM formation in the *ypt3-ki8* mutant. Wild-type (KI51) and *ypt3-ki8* (KI8) cells expressing the FSM marker GFP-Psy1 were sporulated on ME at 28°C for 1 d. Nuclear DNA was stained with Hoechst 33342. Stained cells were classified as follows: type I, containing four small, ring-like structures; type II, containing many dots and aggregates of GFP-Psy1. Bar, 10 μm. (B) The *ypt3-ki8* mutant exhibits temperature-sensitive growth. Wild-type (L968) and *ypt3-ki8* (KI8-1) cells were incubated on YE medium at 25 or 37°C for 4 d. (C) The *ypt3-ki8* allele carries a single nucleotide change (T to C), resulting in replacement of a conserved alanine with valine. Effector and GTP-binding regions are shown in black and gray, respectively. Hs, *Homo sapiens*; Sc, *S.cerevisiae*; Sp, *S. pombe*. (D) The early stage of FSM assembly is disrupted in the *ypt3-ki8* mutant. Wild-type (KI44) and *ypt3-ki8* (KI8-6) cells expressing GFP-Psy1 and mCherry-Atb2, a microtubule marker, were sporulated on ME medium at 28°C for 1–2 d. Chromosomal DNA was stained with Hoechst 33342 and analyzed by fluorescence microscopy. GFP-Psy1 (green), mCherry-Atb2 (red), and Hoechst 33342 (blue) are overlaid in the merged images. Bar, 10 μm. High-magnification images of the region in the white square are shown on the right. Arrowheads indicate GFP-Psy1 dots at sites other than the tips of spindle microtubules. Bar, 1 μm.

| Strain | Temperature (°C) | Frequency of cell types (%) | | |
|---|---|---|---|---|
| | | Normal | Type I | Type II |
| Wild type | 25 | 97.9 | ND | ND |
| | 28 | 95.9 | ND | ND |
| *ypt3-ki8* | 25 | ND | 55.8 | 44.2 |
| | 28 | ND | 35.3 | 64.7 |

Postmeiotic cells were classified as follows: normal, containing four large, ring-like structures; type I, containing four small, ring-like structures; type II, containing many dots and aggregates of GFP-Psy1 (see Figure 1A). ND, not detected. $n > 200$.

**TABLE 1:** Classification of phenotypes of the FSM in postmeiotic cells.

gene was cloned via complementation of its temperature sensitivity and sporulation defect (see *Materials and Methods*). Nucleotide sequencing of the cloned DNA fragment and a complementation test with the *ypt3-i5/its5-1* allele (Cheng *et al.*, 2002) revealed that *spo26*$^+$ encodes the protein Ypt3, an orthologue of *S. cerevisiae* Ypt31/Ypt32 and mammalian Rab11 (Figure 1C; Miyake and Yamamoto, 1990; Urbe *et al.*, 1993; Cheng *et al.*, 2002). Ypt3 is known to regulate the exocytic pathway in fission yeast and is essential for cell viability (Cheng *et al.*, 2002), but its role in sporulation is unclear.

To examine in detail how the *ypt3-ki8* mutation impairs sporulation, we observed assembly of the FSM in the *ypt3-ki8* mutant by using GFP-Psy1. Most wild-type cells displayed GFP-Psy1 fluorescence as circles of uniform brightness, representing FSMs in which a haploid nucleus was already enclosed (Figure 1A and Table 1). In contrast, *ypt3-ki8* exhibited a severe defect in FSM formation. After incubation on sporulation medium at 25°C, about half of the *ypt3-ki8* zygotes contained four small prespores (type I in Figure 1A and Table 1), possibly due to a defect in FSM expansion. The rest of the *ypt3-ki8* zygotes exhibited a more severe phenotype in which a number of aggregates of GFP-Psy1 formed and no FSM was observed (type II in Figure 1A and Table 1). At higher temperature (28°C), the frequency of type II cells increased (Table 1).

Next we examined the initiation of FSM formation in *ypt3-ki8* cells. In wild-type cells, the GFP-Psy1 signal was observed as two cup-like structures at each end of the spindle microtubules, which were visualized by mCherry-labeled Atb2, at metaphase II (Figure 1D and Supplemental Figure S1). In contrast, no GFP-Psy1 signal was observed at ~60% of the spindle poles in *ypt3-ki8* cells (Figure 1D and Supplemental Figure S1). This phenotype is similar to that of mutants of meiotic SPB components such as Spo13 and Spo15 (Ikemoto *et al.*, 2000; Nakase *et al.*, 2008). Taken together, these data indicate that Ypt3 is essential for both the initiation of FSM formation and expansion of the FSM.

To determine the precise identity of the *ypt3-ki8* allele, we isolated the mutant gene from genomic DNA by PCR amplification. Nucleotide sequencing revealed that *ypt3-ki8* resulted from a single nucleotide change (C to T at position 221), which replaced alanine 74 with valine. Alanine 74 is located near the second effector region and is conserved among Rab11/Ypt3 proteins (Figure 1C).

### Ypt3 localizes at the SPB and the FSM during sporulation

A comprehensive mRNA expression study previously revealed that transcription of the *ypt3*$^+$ gene is up-regulated during meiosis (Mata *et al.*, 2002), but Ypt3 protein levels during meiosis are unknown. To ascertain whether the levels of Ypt3 protein mirror those of *ypt3* mRNA, we examined the abundance of GFP-Ypt3 protein during

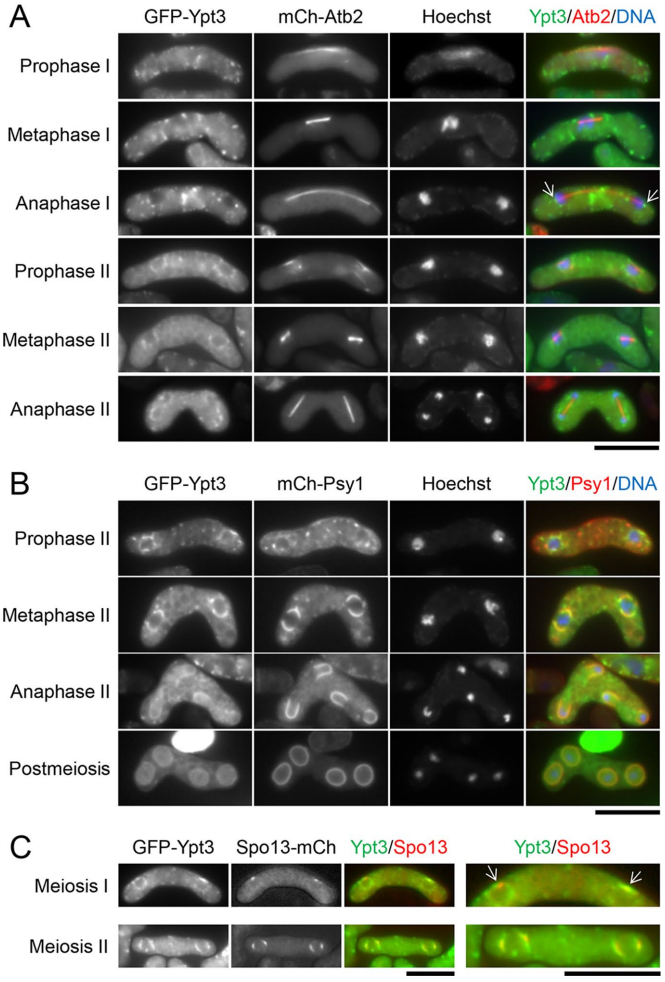


**FIGURE 2:** Localization of Ypt3 during sporulation. (A) Dual observation of Ypt3 and microtubules during sporulation. Homothallic haploid wild-type cells expressing GFP-Ypt3 and mCherry-Atb2 (KI114) were sporulated on ME at 28°C for 1 d. Chromosomal DNA was stained with Hoechst 33342 and analyzed by fluorescence microscopy. GFP-Ypt3 (green), mCherry-Atb2 (red), and Hoechst 33342 (blue) are overlaid in the merged images. Arrows indicate GFP-Ypt3 dots at the spindle poles. (B) Dual observation of Ypt3 and the FSM. Wild-type cells expressing GFP-Ypt3 and mCherry-Psy1 (KI118) were sporulated on ME at 28°C for 1 d. Chromosomal DNA was stained with Hoechst 33342 and analyzed by fluorescence microscopy. GFP-Ypt3 (green), mCherry-Psy1 (red), and Hoechst 33342 (blue) are overlaid in the merged images. (C) Dual observation of Ypt3 and Spo13. Wild-type cells expressing GFP-Ypt3 and Spo13-mCherry (KI132) were sporulated on ME at 28°C for 1 d and analyzed by fluorescence microscopy. GFP-Ypt3 (green) and Spo13-mCherry (red) are overlaid in the merged images. Bars, 10 μm.

sporulation. A strain carrying the *pat1-114* mutation and expressing GFP-Ypt3 was cultured at 34°C to induce synchronous meiosis. Unexpectedly, the abundance of GFP-Ypt3 remained essentially constant after the induction of sporulation (Supplemental Figure S2A).

In vegetative cells, Ypt3 localizes to cell tips and the medial region (Cheng *et al.*, 2002). We next observed the behavior of GFP-Ypt3 during meiosis and sporulation. During prophase I, GFP-Ypt3 was observed as numerous dots dispersed throughout the cytoplasm (Figure 2A). The GFP-Ypt3 dots gradually accumulated around the nucleus before FSM formation (Figure 2, A and B, and

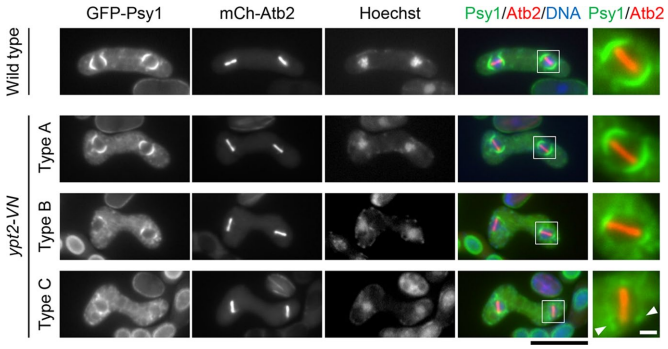


FIGURE 3: Ypt2 is essential for the early stage of FSM formation. The early stage of FSM assembly is disrupted in the *ypt2-VN* mutant. Wild-type (KI173) and *ypt2-VN* (KI168) cells expressing GFP-Psy1 and mCherry-Atb2, a microtubule marker, were sporulated on SSA including 15 μM thiamine at 32°C for 1–2 d. Chromosomal DNA was stained with Hoechst 33342 and analyzed by fluorescence microscopy. GFP-Psy1 (green), mCherry-Atb2 (red), and Hoechst 33342 (blue) are overlaid in the merged images. Stained cells were classified as follows: type A, containing four cup-like structures; type B, containing small FSM-like structures assembled at the spindle poles; type C, containing many dots of GFP-Psy1. Bar, 10 μm. High-magnification images of the region in the white square are shown on the right. Arrowheads indicate GFP-Psy1 dots at sites other than the tips of spindle microtubules. Bar, 1 μm.

| Strain | Frequency of cell types (%) | | |
|---|---|---|---|
| | Type A | Type B | Type C |
| Wild type | 88.1 | 7.1 | 4.8 |
| *ypt2-VN* | 38.2 | 29.4 | 32.4 |

During meiosis II, cells were classified as follows: type A, containing four cup-like structures; type B, containing small FSM-like structures; type C, containing many dots of GFP-Psy1 (see Figure 3). Wild type, $n = 84$; *ypt2-VN*, $n = 34$.

TABLE 2: Classification of phenotypes of the FSM in meiosis II.

Supplemental Figure S3). At metaphase II, GFP-Ypt3 signals almost completely overlapped with the nascent FSM, as labeled by mCherry-Psy1 (metaphase II, Figure 2B). Of interest, GFP-Ypt3 dots were also detected at both ends of the spindle microtubules and overlapped with Spo13-mCherry at anaphase I (Figure 2, A and C). In addition, the GFP-Ypt3 signal was observed at the spindle poles in *spo7*Δ cells, in which FSM formation is completely defective (Nakamura-Kubo *et al.*, 2011), as shown in Figure 6A (see later discussion) and Supplemental Figure S3. These data indicate that Ypt3 localizes to the SPB before FSM formation and support the notion that Ypt3 is involved in the initiation of FSM formation.

### Ypt2 is essential for FSM formation

In *S. cerevisiae*, ScYpt31 and ScYpt32 play important roles in the exocytic pathway together with another Rab GTPase, ScSec4, which functions downstream of ScYpt31 and ScYpt32 (Haubruck *et al.*, 1990). We therefore investigated whether Ypt2, an *S. pombe* orthologue of ScSec4, is involved in FSM formation. It has been shown that Ypt2 functions in a manner similar to ScSec4, because the *ypt2-VN* mutant shows defects in the late stage of the secretory pathway at the restrictive temperature (Craighead *et al.*, 1993). Here GFP-Psy1 dots accumulated around SPBs to form cup-like structures in wild-type cells at metaphase II, but fewer of these structures were observed in *ypt2-VN* cells at a temperature permissive for proliferation (type A in Figure 3 and Table 2). For about one-third of the spindle poles, the accompanying FSM arrested at an early stage (type B in Figure 3 and Table 2), whereas another one-third had no FSM-like structures (type C in Figure 3 and Table 2), indicating that the initiation of FSM formation is apparently defective or delayed in *ypt2-VN*.

To accurately determine the level of Ypt2 protein during sporulation, we cultured a strain carrying the *pat1-114* mutation and expressing GFP-Ypt2 at 34°C to induce synchronous meiosis. As in the case of Ypt3, the abundance of GFP-Ypt2 remained essentially constant after the induction of sporulation (Supplemental Figure S2B), although expression of the *ypt2*$^+$ gene has been reported to be slightly up-regulated during synchronous meiosis (Mata *et al.*, 2002). In vegetative cells, GFP-Ypt2 was detected as dots around the plasma membrane (marked by mCherry-Psy1), especially at growing sites, cell tips, and septation sites (Figure 4A). At an early stage of meiosis (around prophase I), the GFP-Ypt2 signal was dispersed throughout the cytoplasm of the zygote (Figure 4B). At metaphase I, the GFP-Ypt2 signal was predominantly located at the spindle poles and overlapped with mCherry-labeled Spo15 during meiosis I (Figure 4, B and C), indicating that Ypt2 localizes to the SPB. When the cells proceeded to meiosis II, GFP-Ypt2 relocalized to the FSM (Figure 4D). Thus these data support the possibility that Ypt3 and Ypt2 function in the same pathway as the one that regulates the initiation of FSM biogenesis.

### Localization of Ypt2 and Ypt3 depends on the meiotic SPB component Spo13

Generally, localization of Rab on the correct membrane is dependent on a specific guanine nucleotide exchange factor (GEF; Blümer *et al.*, 2013; Cabrera and Ungermann, 2013). In *S. pombe*, two proteins, Sec2 (an orthologue of *S. cerevisiae* Sec2) and Spo13 (which has homology to the ScSec2 GEF domain), are believed to act as GEFs for Ypt2 (Figure 5A; Yang and Neiman, 2010). Because Spo13 is a meiosis-specific SPB component (Nakase *et al.*, 2008), we hypothesized that Spo13 might recruit Ypt2 to the SPB. To confirm this, we observed the behavior of GFP-Ypt2 and Spo13-mCherry simultaneously. At an early stage of meiosis I, the Spo13-mCherry signal was detected on the SPB as dots (Figure 5B; Nakase *et al.*, 2008), whereas the GFP-Ypt2 signal was diffused throughout the cytoplasm (Figure 5B). Subsequently, the GFP-Ypt2 signal was almost completely overlapped by Spo13-mCherry (Figure 5B), indicating that Spo13 is recruited to the SPB before Ypt2. This result was confirmed by live-cell imaging (Supplemental Figure S4A). During FSM formation, GFP-Ypt2 relocalized to the FSM, whereas Spo13-mCherry persisted on the SPB (Figure 5B).

To determine whether localization of Ypt2 at the SPB is dependent on Spo13, we observed the localization of Ypt2 in *spo13*Δ cells. Of interest, GFP-Ypt2 fluorescence was not detected at the spindle poles in *spo13*Δ cells but was dispersed throughout the cytoplasm (Figure 5C and Supplemental Figure S4B). To examine whether this defect in Ypt2 localization at the SPB is a consequence of the defect in FSM formation, we observed the behavior of GFP-Ypt2 in *spo7*Δ cells. As shown in Figure 5C and Supplemental Figure S4B, GFP-Ypt2 dots at the SPB were observed in *spo7*Δ cells. Thus these data demonstrate that localization of Ypt2 is dependent on the meiotic SPB component Spo13. Conversely, localization of Spo13-GFP was not affected by the *ypt2* mutation (Supplemental Figure S5A).

Of note, Spo13 was also required for localization of Ypt3 at the SPB (Figure 6A and Supplemental Figure S3). The GFP-Ypt3 signal

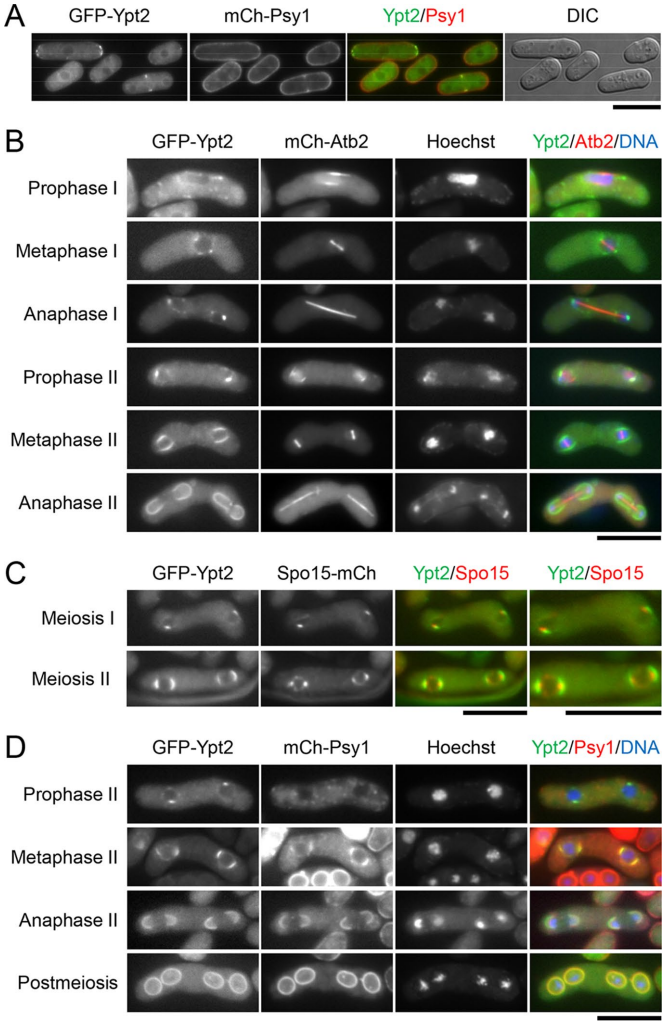


FIGURE 4: Expression and localization of Ypt2 during sporulation. (A) Dual observation of Ypt2 and the plasma membrane during vegetative growth. Wild-type cells expressing GFP-Ypt2 and mCherry-Psy1 (KI78) were cultured on YE medium at 28°C for 1 d and analyzed by fluorescence microscopy. GFP-Ypt2 (green) and mCherry-Psy1 (red) are overlaid in the merged images. (B) Dual observation of Ypt2 and microtubules during sporulation. Wild-type cells expressing GFP-Ypt2 and mCherry-Atb2 (KI109) were sporulated on ME at 28°C for 1 d. Chromosomal DNA was stained with Hoechst 33342 and analyzed by fluorescence microscopy. GFP-Ypt2 (green), mCherry-Atb2 (red), and Hoechst 33342 (blue) are overlaid in the merged images. (C) Dual observation of Ypt2 and Spo15. Wild-type cells expressing GFP-Ypt2 and Spo15-mCherry (KI162) were sporulated on ME at 28°C for 1 d and analyzed by fluorescence microscopy. GFP-Ypt2 (green) and Spo15-mCherry (red) are overlaid in the merged images. (D) Dual observation of Ypt2 and the FSM. Wild-type cells expressing GFP-Ypt2 and mCherry-Psy1 (KI78) were sporulated on ME at 28°C for 1 d. Chromosomal DNA was stained with Hoechst 33342 and analyzed by fluorescence microscopy. GFP-Ypt2 (green), mCherry-Psy1 (red), and Hoechst 33342 (blue) are overlaid in the merged images. Bars, 10 μm.

was detected in a similar location in *ypt2-VN* and wild-type cells (Supplemental Figure S5B), indicating that recruitment of Ypt3 to the SPB is independent of Ypt2. Because Ypt3 is known to be concentrated at secretory vesicles or endosomes (Cheng *et al.*, 2002), we next investigated the behavior of secretory vesicles during meiosis using GFP-tagged Syb1, a homologue of mammalian synaptobrevin (Edamatsu and Toyoshima, 2003; Kita *et al.*, 2004). GFP-Syb1 signals were detected as numerous dots, as described previously (Yamaoka *et al.*, 2013), and some were also detected at the spindle poles. As in the case of Ypt3 and Ypt2, GFP-Syb1 was not observed at the SPB in *spo13*Δ cells but was in *spo7*Δ cells (Figure 6B and Supplemental Figure S6). These data suggest that secretory vesicles are recruited to the SPB before formation of the FSM. In the *ypt3-ki8* mutant, GFP-Syb1 localized on the SPB as in wild-type cells (Figure 6B and Supplemental Figure S6). Given that the *ypt3-ki8* mutant exhibits defect in FSM formation, this observation suggests that the Ypt3-ki8 protein has the ability to deliver secretory vesicles to the SPB but not to fuse them to the target membrane.

### Physical interaction of Ypt3 with Sec2 and Spo13

In budding yeast, ScSec2, the GEF for ScSec4, is also an effector for ScYpt32 (Ortiz *et al.*, 2002). Although Spo13 and Sec2 bound to inactive Ypt2 (Supplemental Figure S7) and are believed to act as Ypt2 GEFs in *S. pombe* (Yang and Neiman, 2010), they have not been identified as Ypt3 effectors. To evaluate the interaction of Ypt3 with Spo13 and/or Sec2 in more detail, we performed in vitro binding experiments with purified proteins. Recombinant GST-Ypt3 was immobilized on glutathione-Sepharose beads, which were then loaded with GDP or GTPγS, a GTP analogue. The beads were incubated with the lysate of cells expressing Spo13-3xGFP or Sec2-GFP and then collected and washed. Incubation of the beads with GST alone was used as a control for nonspecific binding. As shown in Figure 7A, Sec2 interacted preferentially with GST-Ypt3 bound to GTPγS. Typically, all GTPase effectors interact specifically with the GTP-bound form of a GTPase (Grosshans *et al.*, 2006a,b; Hutagalung and Novick, 2011); thus the pull-down assay suggested that Sec2 is an effector of Ypt3 GTPase. In contrast, Spo13-3xGFP interacted with both forms of Ypt3 to a similar extent (Figure 7B). A similar pattern of interaction was detected when HA-Spo13 was used in the assay (Supplemental Figure S8). Therefore it was not possible to determine whether Spo13 acts as an effector of Ypt3, at least by in vitro binding assays.

### Localization of Sec2 during sporulation

To investigate the role of Sec2 in FSM formation, we observed localization of Sec2-GFP during this process. Consistent with previous data (Matsuyama *et al.*, 2006), Sec2-GFP was detected as dots at growing sites, cell tips, and the medial region during vegetative growth (Figure 8A). Similar to Ypt3 and Ypt2, Sec2-GFP was detected as numerous dots during meiosis I (Figure 8B). Some Sec2-GFP signals then accumulated on the spindle poles as meiosis proceeded, and an intense dot was observed at the center of each FSM, especially in anaphase II (Figure 8, B and C, and Supplemental Figure S9, A–C). After meiosis had completed, the concentrated Sec2-GFP dots were observed diffusely on the closed FSMs. In *spo2*, *spo7*, *spo13*, and *spo15* mutant cells, concentrated Sec2-GFP signals were observed at the spindle poles (Supplemental Figure S9D).

In *S. cerevisiae*, active ScYpt32 recruits ScSec2 to its specific membrane, where ScSec2 activates ScSec4 to associate with the membrane (Mizuno-Yamasaki *et al.*, 2010). We therefore observed the behavior of Sec2-GFP in the *ypt3-ki8* mutant. In vegetatively growing cells, the Sec2-GFP dots that localized at the growing sites appeared to be reduced in *ypt3-ki8* cells, whereas their intensity in the cytoplasm increased (Supplemental Figure S10A). Similarly, Sec2-GFP dots at the spindle poles were significantly reduced in *ypt3-ki8* cells during meiosis (Figure 9A). Taken together, these data indicate that recruitment of Sec2 to the SPB is dependent on Ypt3 but not on known meiotic SPB components such as Spo2, Spo7, Spo13, and Spo15.

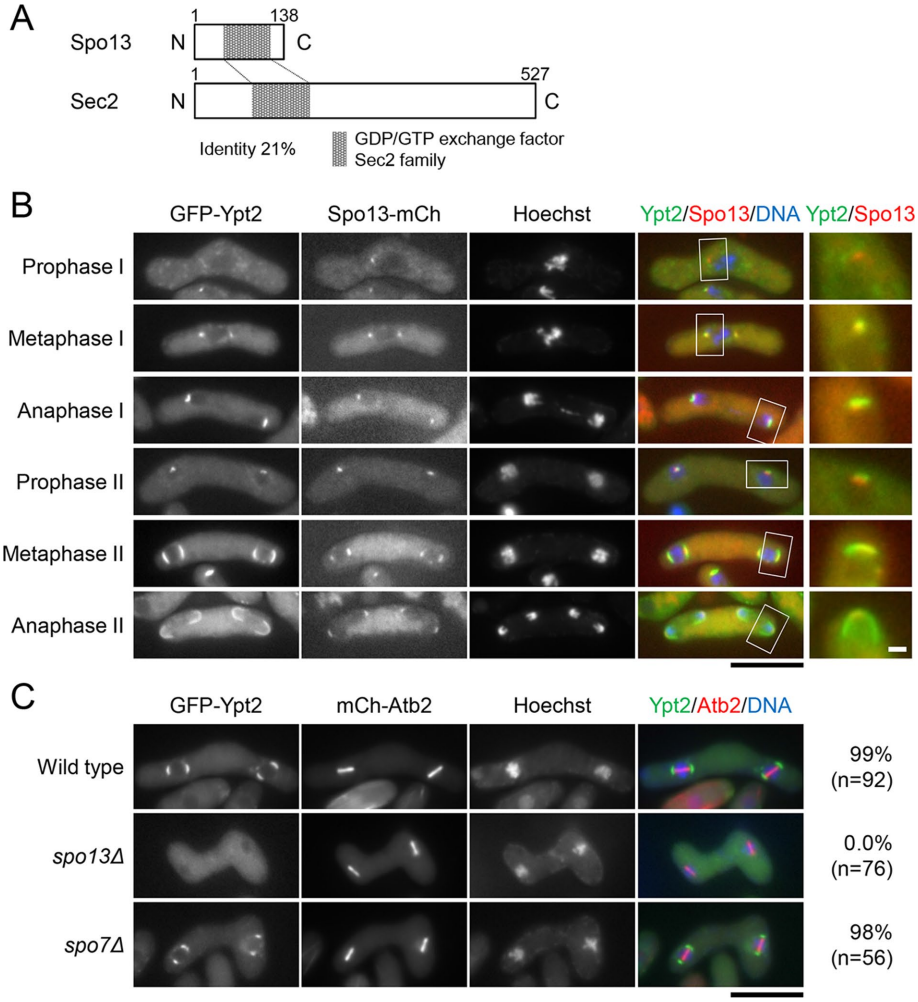


FIGURE 5: Ypt2 localizes at the SPB in a Spo13-dependent manner. (A) Schematic illustration of Spo13 and Sec2. The predicted GEF domain is indicated by a gray box. (B) Dual observation of Ypt2 and Spo13. Wild-type cells expressing GFP-Ypt2 and Spo13-mCherry (KI130) were sporulated on ME at 28°C for 1 d. Chromosomal DNA was stained with Hoechst 33342 and analyzed by fluorescence microscopy. GFP-Ypt2 (green), Spo13-mCherry (red), and Hoechst 33342 (blue) are overlaid in the merged images. Bar, 10 μm. High-magnification images of the region in the white square are shown on the right. Bar, 1 μm. (C) Localization of Ypt2 in *spo13*Δ and *spo7*Δ. Wild-type (KI109), *spo13*Δ (KI97), and *spo7*Δ (KI96) strains expressing GFP-Ypt2 and mCherry-Atb2 were sporulated on ME at 28°C for 1 d. Chromosomal DNA was stained with Hoechst 33342 and analyzed by fluorescence microscopy. GFP-Ypt2 (green), mCherry-Atb2 (red), and Hoechst 33342 (blue) are overlaid in the merged images. Cells at other stages are shown in Figure 4B (wild type) and Supplemental Figure S4B (*spo13*Δ and *spo7*Δ). The frequency of GFP-Ypt2 signals at the spindle pole during meiosis II is indicated on the right. Bar, 10 μm.

### The exocyst is also localized at the meiotic SPB and required for FSM formation

The exocyst, a highly conserved complex composed of eight subunits (Sec3, Sec5, Sec6, Sec8, Sec10, Sec15, Exo70, and Exo84), tethers secretory vesicles to the plasma membrane before exocytic membrane fusion (Heider and Munson, 2012). In budding yeast, components of the exocyst are recruited to secretory vesicles by GTP-bound ScSec4 (Guo *et al.*, 1999; Boyd *et al.*, 2004). To examine whether the exocyst is involved in formation of the FSM, we observed Sec8-GFP behavior during sporulation. During prophase I, the Sec8-GFP signal was observed as peripheral dots at the plasma membrane in wild-type cells. These dots then diffused and gradually appeared at the SPBs during anaphase I (Supplemental Figure S11A). The SPB localization of Sec8 was also detected in *spo7*Δ and *spo13*Δ cells (Supplemental Figure S11B), indicating that the exocyst is recruited to the SPB independently of Spo7 and Spo13.

Next we observed FSM formation in the *sec8-1* mutant that shows defects in exocytosis (Wang *et al.*, 2002). About one-third of the postmeiotic *sec8-1* cells contained more than four small spore-like structures (Supplemental Figure S11, C and D), suggesting that Sec8 has a role in FSM formation. However, we did not observe a defect in the initiation of FSM formation in this mutant.

### Ypt3 is required for SPB integrity during sporulation

Finally, we examined whether localization of Spo13 at the SPB is dependent on Ypt3. As shown in Figure 9B, Spo13-GFP dots were essentially detected at the spindle poles in *ypt3-ki8* cells; however, a considerable fraction was localized at sites other than spindle poles. This defect in Spo13-GFP localization in *ypt3-ki8* is reminiscent of that seen in a mutant of Spo20, a phosphatidylinositol/phosphatidylcholine-transfer protein. In the *spo20-H6* mutant, several SPB-like structures called pseudo-SPBs are separated from the spindle poles during the progression of meiosis. The pseudo-SPBs contain various SPB components, including essentially Spo13 and Spo15, but do not contain Alp4, a component of the γ-tubulin complex (Nakase *et al.*, 2004). We therefore determined whether the extra Spo13-GFP dots observed in the *ypt3-ki8* mutant are related to pseudo-SPBs. As shown in Supplemental Figure S12, A–D, whereas Spo15-GFP was separated from the spindle poles, most Alp4 localized correctly at the spindle poles in the *ypt3-ki8* mutant. These results suggest that, similar to Spo20, Ypt3 plays a role in maintaining the structural integrity of the meiotic SPB but not in recruiting meiotic SPB components to the SPB.

## DISCUSSION

Previous studies determined that various components of the membrane trafficking pathway play pivotal roles in FSM formation (Neiman, 1998, 2011; Nakase *et al.*, 2001; Nakamura-Kubo *et al.*, 2003; Nakamura *et al.*, 2005). In this study, we isolated a novel *spo* mutant, *spo26/ypt3*, which exhibits a severe defect in FSM formation. *ypt3*$^+$ encodes an orthologue of mammalian Rab11 GTPase, a master regulator of the post-Golgi secretory pathway. We also examined the role of Ypt2, another Rab protein involved in post-Golgi membrane vesicle transport, in the formation of the FSM. Our results demonstrate that both Rab GTPases are important in the initiation of FSM formation. The component of the SPB that provides a key function as the nucleation site for the FSM has been unknown. We found that first Ypt2 and then Ypt3 are localized to the SPB before formation of the FSM and are important in the initiation of FSM formation. Our results suggest that Ypt2 and

Ypt3 are potential proteins that anchor the membrane at the meiotic SPB.

During prophase I, GFP-Ypt2 signals were observed as many dots throughout the cytoplasm (Figure 4B), suggesting that Ypt2 is associated with membrane vesicles. At metaphase I, however, the GFP-Ypt2 signal was observed predominantly at the SPB, but some dots were dispersed homogeneously in the cytoplasm (Figure 4B). Furthermore, previous electron microscopy data showed that no obvious membrane- and vesicle-like structures are found on the SPB at this stage (Hirata and Tanaka, 1982; Hirata and Shimoda, 1994). Thus we presume that, during meiosis I, Ypt2 localizes to the SPB via Spo13 without associating with membrane vesicles. This is consistent with the results of the yeast two-hybrid assay, which showed that Spo13 preferentially interacts with Ypt2 in the GDP-bound form (Supplemental Figure S7). A GDP dissociation inhibitor (GDI) would bind to the Rab in GDP-bound form and inhibit the GDP/GTP exchange and the membrane association of the Rab protein. *S. pombe* is known to possess a single GDI, Gdi1. Of interest, Gdi1 interacts with Ypt2 physically and is up-regulated during meiosis (Mata *et al.*, 2002; Ma *et al.*, 2006). At meiosis I, therefore, Gdi1 might interact with Ypt2 and inhibit its association with the membrane.

Unlike Spo13, Sec2 does not seem to be essential for recruitment of Ypt2 to the SPB, because Ypt2 localized to the SPB in *ypt3-ki8* cells, whereas Sec2 did not (Figure 9, A and C, and Supplemental Figures S4B and S9D). Moreover, Spo13 preferentially interacts with the nucleotide-free form of ScSec4. In vitro, the GEF activity of Spo13 is not strong relative to that of the GEF domain of ScSec2 (Yang and Neiman, 2010). One possibility is that Sec2 and Spo13 have distinct roles in FSM formation: Sec2 may function mainly as a GEF for Ypt2, whereas Spo13 may function as a scaffold for Ypt2 at the SPB. In support of this possibility, overproduction of Sec2 did not complement the sporulation defect of *spo13*Δ. However, a *spo13* mutant defective in GEF activity shows compromised initiation of FSM formation (Yang and Neiman, 2010). Therefore Spo13 may be required for both the localization and activation of Ypt2. It is unclear how Sec2 is involved in FSM formation. Isolation of a *sec2* allele will be required to address the detailed role of Sec2 in FSM formation.

As mentioned earlier, the Rab cascade plays an important role in the exocytic pathway in *S. cerevisiae*. Several lines of evidence suggest that the corresponding Rab cascade (i.e., Ypt3–Sec2–Ypt2) also functions in the *S. pombe* exocytic pathway. First, Sec2 is essential for vegetative growth (Hayles *et al.*, 2013). Second, both Ypt3 and Ypt2 are involved in the exocytic pathway (Haubruck *et al.*, 1990; Craighead *et al.*, 1993; Cheng *et al.*, 2002). Third, Sec2 and Ypt2 are not localized at the cell tip or middle part of the dividing cell in *ypt3* (Supplemental Figure S10). Fourth, Sec2 associated with Ypt3 preferentially in its GTP-bound form (Figure 7). During sporulation, all of these proteins localize to the SPB before formation of the FSM initiates.

Figure 10 illustrates our working hypothesis in which Rabs and GEFs regulate the initiation of FSM formation. At the end of prophase I, Spo13 is expressed and localized to the SPB, where it recruits and anchors Ypt2. Next Ypt3-containing vesicles (i.e., secretory vesicles) are recruited to the SPB, dependent on Spo13. Electron microcopy has shown that membrane vesicles are located near the modified SPB in *spo7*Δ cells, in which Ypt2 and Ypt3 can localize at the SPB, whereas no vesicles are observed in *spo13*Δ cells (Nakase *et al.*, 2008; Nakamura-Kubo *et al.*, 2011). Coincidentally, Sec2 and the exocyst localize to the SPB independently of Spo13 (Supplemental Figures S9D and S11, A and B). In *S. cerevisiae*, ScSec2 is recruited to Golgi-derived vesicles by ScYpt32 and activates ScSec4, which in turn recruits the exocyst to interact with both ScSec2 and ScSec4 (Medkova *et al.*, 2006). However, neither the SPB localization of Sec2 nor that of the exocyst is dependent on Spo13 (Supplemental Figure S9D). In *S. pombe*, the exocyst localizes to the division site dependent on F-actin but independent of the secretory pathway during vegetative growth (Wang *et al.*, 2002).

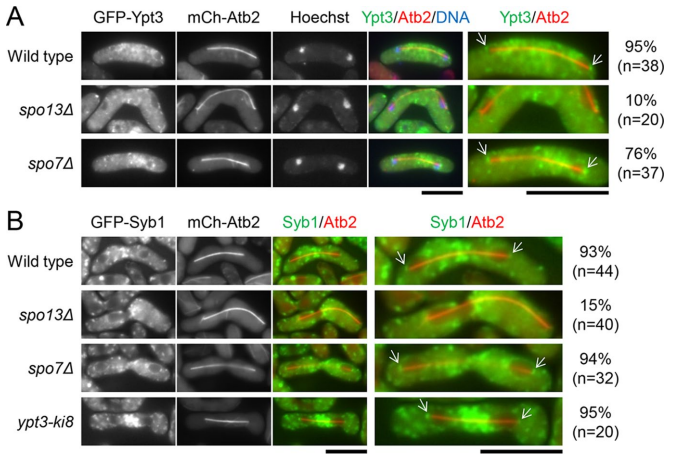


FIGURE 6: Secretory vesicles are recruited to the SPB in a Spo13-dependent manner. (A) Localization of Ypt3 in *spo13*Δ and *spo7*Δ in anaphase I. Wild-type (KI70), *spo13*Δ (KI99), and *spo7*Δ (KI98) cells expressing GFP-Ypt3 and mCherry-Atb2 were sporulated on ME at 28°C for 1 d. Chromosomal DNA was stained with Hoechst 33342 and analyzed by fluorescence microscopy. GFP-Ypt3 (green), mCherry-Atb2 (red), and Hoechst 33342 (blue) are overlaid in the merged images. Cells in meiosis II are shown in Supplemental Figure S3. (B) Localization of Syb1 in *spo13*Δ, *spo7*Δ, and *ypt3-ki8* in anaphase I. Wild-type (KI248), *spo13*Δ (KI254), *spo7*Δ (KI252), and ypt3-ki8 (KI8-51) cells expressing GFP-Syb1 and mCherry-Atb2 were sporulated on ME at 28°C for 1 d and analyzed by fluorescence microscopy. GFP-Syb1 (green) and mCherry-Atb2 (red) are overlaid in the merged images. Cells in meiosis II are shown in Supplemental Figure S6. Arrows indicate GFP dots at the spindle poles. The frequency of GFP dots at the spindle pole during late anaphase I is also indicated. Bars, 10 μm.

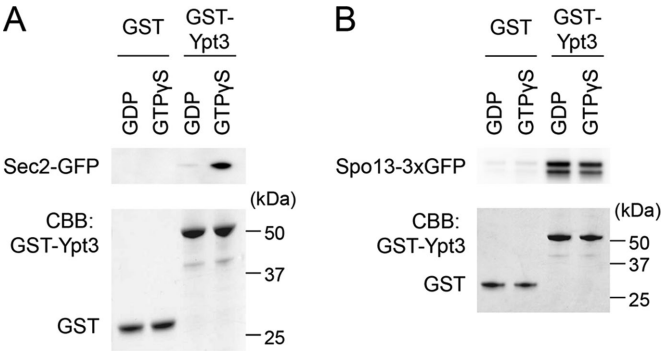


FIGURE 7: Physical interaction of Spo13 with Ypt3. GST or GST-Ypt3 was expressed in *E. coli* cells and immobilized on glutathione-Sepharose beads. After preloading with either GDP or GTPγS, the beads were incubated with the lysate of yeast cells (TN104) overexpressing Sec2-GFP (A) or Spo13-3xGFP (B) from plasmid pKI202 or pKI201, respectively. The beads were precipitated by centrifugation, washed, and then subjected to immunoblotting with anti-GFP antibody (top). SDS–PAGE gels were stained with Coomassie brilliant blue (CBB) as a loading control (bottom).

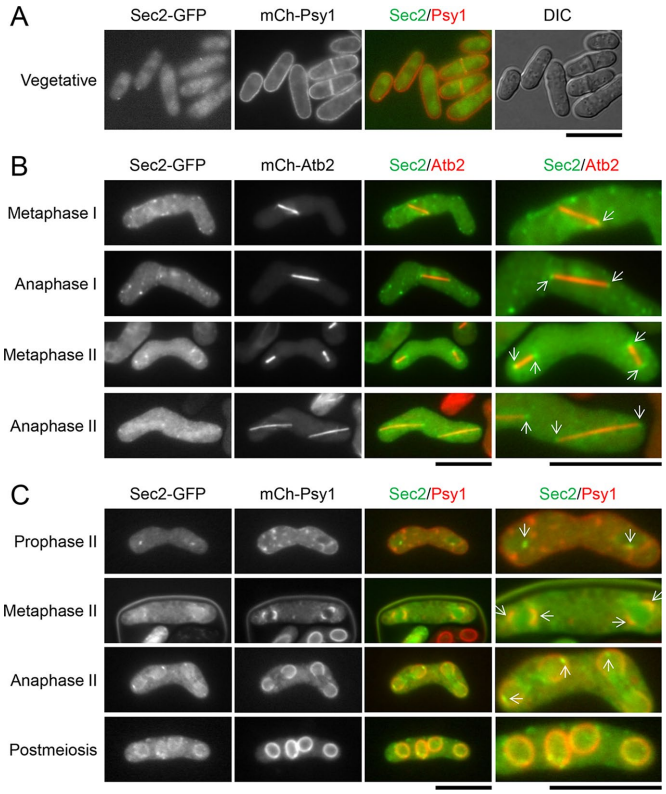


FIGURE 8: Localization of Sec2. (A) Localization of Sec2 during vegetative growth. Wild-type (KI129) cells expressing Sec2-GFP and mCherry-Psy1 were cultured on YE medium at 25°C for 1 d. Sec2-GFP (green) and mCherry-Psy1 (red) are overlaid in the merged images. (B) Dual observation of Sec2 and microtubules. Wild-type cells (KI34) expressing Sec2-GFP from plasmid (pKI33) and mCherry-Atb2 were sporulated on SSA including 15 μM thiamine at 28°C for 1 d and analyzed by fluorescence microscopy. Sec2-GFP (green) and mCherry-Atb2 (red) are overlaid in the merged images. Arrows indicate Sec2-GFP dots at the spindle poles. (C) Dual observation of Sec2 and the FSM. Wild-type cells (KI53) expressing Sec2-GFP from plasmid (pKI33) and mCherry-Psy1 were sporulated on SSA including 15 μM thiamine at 28°C for 1 d and analyzed by fluorescence microscopy. Sec2-GFP (green) and mCherry-Psy1 (red) are overlaid in the merged images. Arrows indicate Sec2-GFP dots on the FSM. Bars, 10 μm.

Therefore it is possible that the SPB localization of the exocyst and its potential binding partner Sec2 may depend on F-actin, which concentrates around the nucleus before FSM formation starts (Petersen *et al.*, 1998; Toya *et al.*, 2001). We previously showed that Psy1, the fission yeast orthologue of syntaxin 1, is selectively internalized by endocytosis and relocalized to the nascent FSM (Kashiwazaki *et al.*, 2011). Given that Syb1 is already localized to the SPB (Figure 6B and Supplemental Figure S6), one possibility is that the Rab cascade (Ypt3–Sec2–Ypt2 and/or Ypt3–Spo13–Ypt2) may regulate fusion between secretory vesicles, including Syb1 and endocytic vesicles containing Psy1 on the SPB. In support of this possibility, we identified *psy1* and *syb1* mutants in which FSM formation is completely inhibited (unpublished data). However, the exocyst mutant *sec8-1* did not show a severe defect in the initiation of FSM formation (Supplemental Figure S11, C and D). We suggest that this is due to the leakiness of the *sec8-1* allele. Alternatively, membrane tethering by the exocyst might not be essential for the initiation of FSM formation as in the case of polarized growth in *S. pombe* (Wang *et al.*, 2002).

The Rab and GEF proteins are recruited to the SPB at meiosis I, but FSM formation is initiated at meiosis II. How are the Rab and GEF proteins activated for the initiation of FSM formation? In mammalian cells, primary ciliogenesis—formation of the ciliary membrane—starts in the vicinity of the pericentrosome. The ciliary membrane also develops by membrane vesicle fusion. Rab11, Rabin8, and Rab8, corresponding to Ypt3, Sec2, and Ypt2, respectively, are involved in the formation of this membrane (Yoshimura *et al.*, 2007; Knödler *et al.*, 2010; Nachury *et al.*, 2010; Feng *et al.*, 2012). Under conditions of serum starvation, before formation of the ciliary membrane, Rabin8 is recruited to the membrane vesicle dependent on Rab11 and is transported to the centrosome (Westlake *et al.*, 2011; Chiba *et al.*, 2013). Ultimately, Rab8 localizes to the centrosome in a Rabin8-dependent manner, facilitating the docking and fusion of vesicles and forming the ciliary membrane (Nachury *et al.*, 2007; Westlake *et al.*, 2011). These facts imply that the regulation of precursor vesicle fusion by Sec4 homologues on the SPB and centrosome has been conserved throughout evolution. The nuclear Dbf2-related (NDR) kinase 2 phosphorylates Rabin8, and this phosphorylation event is crucial for ciliogenesis (reviewed in Hergovich *et al.*, 2006; Chiba *et al.*, 2013). Of interest, *S. pombe* expresses a meiosis-specific NDR kinase, Mug27 (also known as Ppk35 and Slk1; Ohtaka *et al.*, 2008; Pérez-Hidalgo *et al.*, 2008; Westlake *et al.*, 2011; Chiba *et al.*, 2013). Although *mug27* deletion reduces spore size, the mutant cells can initiate FSM formation. Therefore the regulation of Rabin8/Spo13/Sec2 may essentially differ between formation of the FSM and formation of the ciliary membrane. Further work is required to identify the molecules that regulate the Rab cascade in meiosis-specific functions.

## MATERIALS AND METHODS

### Yeast strains and culture conditions

The fission yeast strains used in this study are listed in Supplemental Table S1. Strains expressing GFP- or mCherry-tagged proteins were constructed by crossing two strains and/or by integration of the plasmid DNA listed in Supplemental Table S2. The tagged proteins were deemed functional on the basis of their ability to rescue the defects of the mutants (unpublished data). Vegetative cultures were propagated in complete (yeast extract [YE]) or synthetic (synthetic defined [SD], modified minimal medium [MB], or minimal medium plus nitrogen [MM+N]) medium supplemented with nutrients essential for auxotrophic strains (Egel and Egel-Mitani, 1974; Moreno *et al.*, 1990; Okazaki *et al.*, 1990). For sporulation, cells precultured in YE, SD, or MM+N were incubated in malt extract medium (ME) or synthetic sporulation medium (SSA or MM-N), respectively. Synchronous meiosis was induced in diploid strains harboring the *pat1-114* allele by a temperature shift as previously described (Iino *et al.*, 1995).

### Plasmids

The plasmids used in this study are listed in Supplemental Table S2. Genomic DNA encoding *ypt3*, *ypt2*, and *sec2* was amplified by PCR from L968 genomic DNA or the genomic library pTN-L1 (Nakamura *et al.*, 2001) and used to construct plasmids carrying the respective genes. The cDNA clone of *ypt3*$^+$, FYC239, was provided by the Yeast Genetic Resource Center (yeast.lab.nig.ac.jp/nig/index_en.html). The *ypt3*$^+$ cDNA was amplified and cloned into pGEX-KG (Guan and Dixon, 1991) at a *Bam*HI–*Eco*RI site to construct pKI34, pGEX-KG (ypt3). A GTP- or GDP-locked mutation was introduced into *ypt2* (Q68L or S18V, respectively) by site-directed mutagenesis using the two-step PCR method, and the products were cloned into pGADT7 or pGBKT7 (Clontech Laboratories, Mountain View, CA).

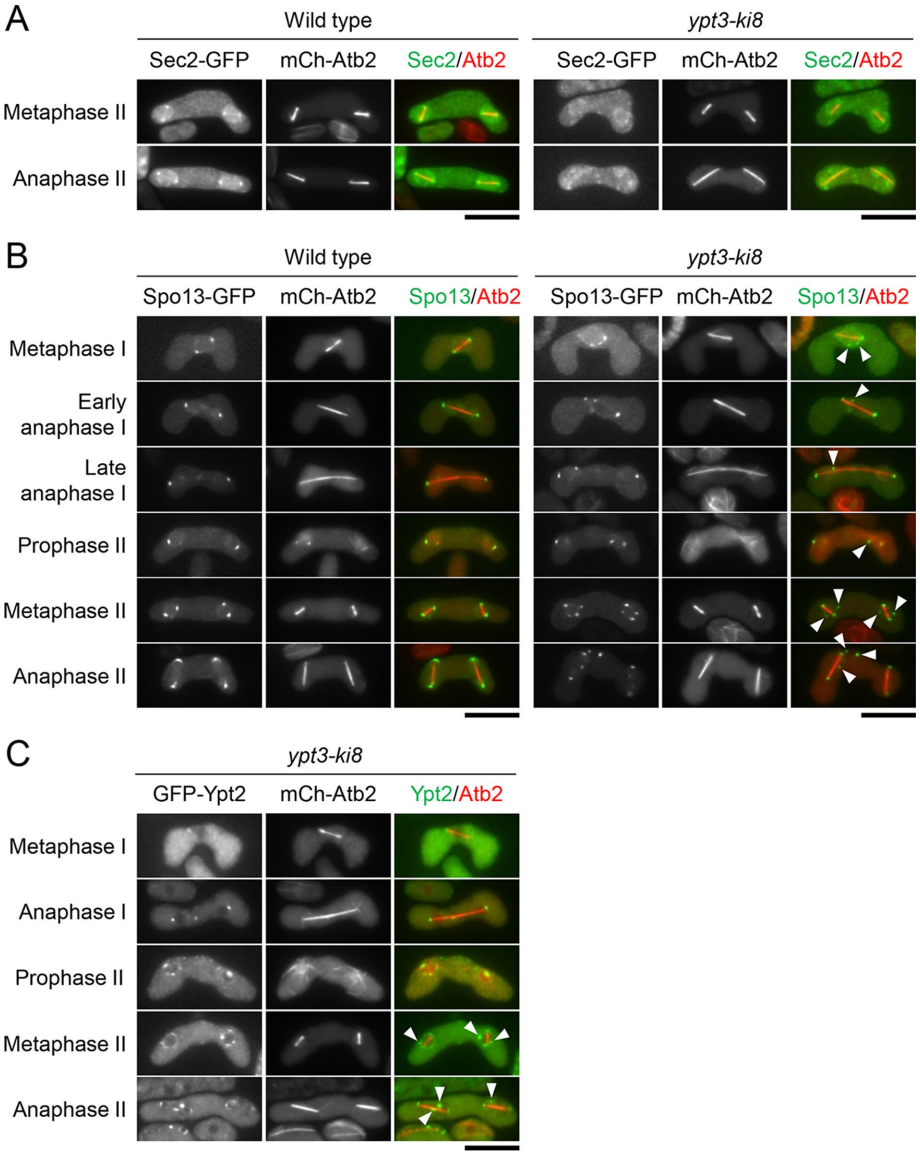


FIGURE 9: Localization of Sec2, Spo13, and Ypt2 in the *ypt3-ki8* mutant. (A) Localization of Sec2 in *ypt3-ki8* during sporulation. Wild-type (KI34) and *ypt3-ki8* (KI8-7) cells expressing Sec2-GFP from plasmid (pKI33) and mCherry-Atb2 were sporulated on SSA including 15 μM thiamine at 28°C for 1–2 d and analyzed by fluorescence microscopy. Sec2-GFP (green) and mCherry-Atb2 (red) are overlaid in the merged images. (B) Localization of Spo13 in *ypt3-ki8* during sporulation. Wild-type (KI112) and *ypt3-ki8* (KI8-17) cells expressing Spo13-GFP and mCherry-Atb2 were sporulated on ME at 28°C for 1–2 d and analyzed by fluorescence microscopy. Spo13-GFP (green) and mCherry-Atb2 (red) are overlaid in the merged images. Arrowheads indicate Spo13-GFP dots at sites other than the tips of spindle microtubules. (C) Localization of Ypt2 in *ypt3-ki8* during sporulation. *ypt3-ki8* cells expressing GFP-Ypt2 and mCherry-Atb2 (KI8-16) were sporulated on ME at 28°C for 2 d and analyzed by fluorescence microscopy. Wild-type cells are shown in Figure 4B. Arrowheads indicate GFP-Ypt2 dots other than the tips of spindle microtubules. Bars, 10 μm.

Further information on the plasmids constructed in this study is on the National BioResource Project Yeast website (yeast.lab.nig.ac.jp/nig.v2.1/index_en.html).

### Isolation of sporulation-deficient mutants

Cells harboring GFP-Psy1, a fluorescent marker of the FSM, were mutagenized with DNA-alkylating agents as follows. TN414 cells were treated with *N*-methyl-*N*′-nitro-*N*-nitrosoguanidine. The cells were spread on ME plates to induce sporulation. After incubation at 28°C for 5 d, colonies with a defect in ascospore formation were detected by exposure to iodine vapor, which stains fission yeast colonies that have sporulated normally. Nonstained cells were observed under a fluorescence microscope to screen for *spo* mutants that completed mating and meiotic divisions but showed aberrant FSM formation.

### Cloning and identification of *spo26*$^{+}$ gene

The *spo26* mutant KI8 cells transformed with the *S. pombe* genomic library pTN-L1 (Nakamura *et al.*, 2001) containing partial *Sau*3AI fragments constructed in the multicopy plasmid pAL-KS (Tanaka *et al.*, 2000) were spread on SD and incubated for 4 d at 37°C. Viable clones that recovered the temperature sensitivity, which is genetically linked to the sporulation defect, were screened. The isolated clones were then incubated on SSA for 2 d at 28°C, and suppression of the *spo* mutation was verified by microscopy.

### Fluorescence microscopy

Proteins were visualized by fusion to GFP or mCherry. The nuclear chromatin region was stained with bisbenzimide H33342 fluorochrome trihydrochroride (Hoechst 33342). Living cells were observed under a fluorescence microscope (model BX51; Olympus, Tokyo, Japan), and images were obtained by using a cooled charge-coupled device camera (ORCA-R2; Hamamatsu Photonics, Hamamatsu, Japan) controlled by AQUACOSMOS software (Hamamatsu Photonics). The time-lapse observation was performed as follows. Cells were incubated on ME at 28°C for 1 d. After conjugation, cells were inoculated to MM-N medium containing 15 μM thiamine on a cell culture dish with a glass bottom (Greiner Bio-One, Frickenhausen, Germany) and observed under a fluorescence microscope (model IX71; Olympus) as described in Nakamura *et al.* (2008). Images were processed with ImageJ (National Institutes of Health, Bethesda, MD).

### Western blotting

Proteins were resolved by SDS–PAGE and then transferred to a polyvinylidene difluoride membrane (Immobilon-P; Merck Millipore, Darmstadt, Germany). Blots were probed with a rat anti-GFP antibody (a gift from S. Fujita, Mitsubishi Kagaku Institute of Life Sciences), the anti–α-tubulin antibody TAT-1 (Woods *et al.*, 1989), or an anti-hemagglutinin antibody (3F10; Roche Diagnostics, Basel, Switzerland) at a dilution of 1:5000. Immunoreactive bands were revealed by ECL Select chemiluminescence (GE Healthcare, Little Chalfont, United Kingdom) with horseradish peroxidase–conjugated goat anti-rat immunoglobulin G (Biosource International, Camarillo, CA) or sheep anti-mouse IgG (GE Healthcare).

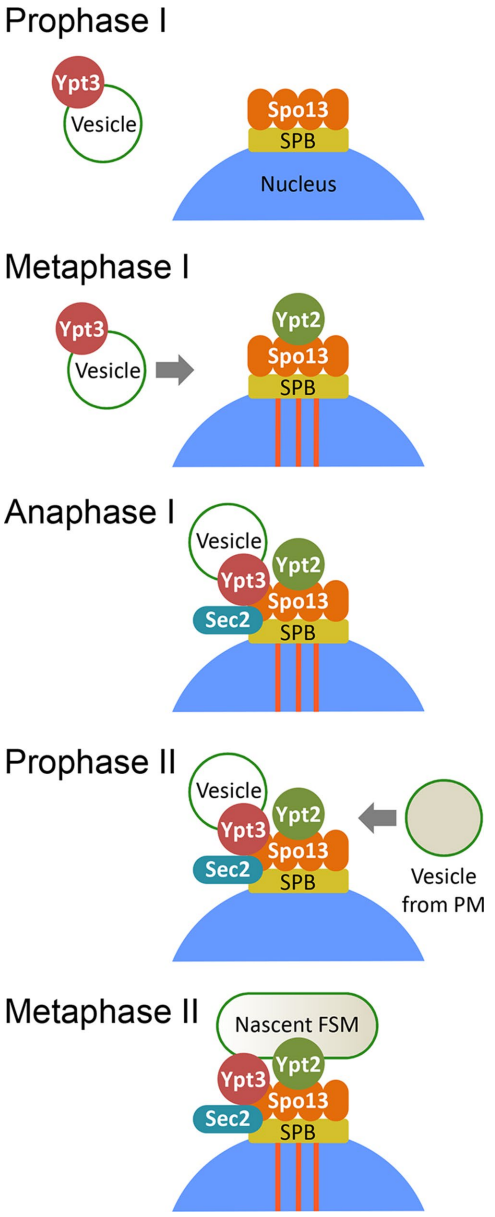


FIGURE 10: Working model of the initiation of FSM formation.

### Pull-down assay

Recombinant glutathione *S*-transferase (GST) and GST-Ypt3 were purified as follows. *Escherichia coli* cells (BL21 Rosetta) harboring pTN174 or pKI34 were grown at 37°C overnight. The culture was diluted 1:1000 in 200 ml of Luria–Bertani broth (LB) and incubated at 37°C for 2 h. After incubation, expression was induced by the addition of 0.1 mM isopropyl-β-D-thiogalactoside, and the culture was incubated at 17°C for 17 h. Cells were harvested, washed, and suspended in 10 ml of TES buffer (20 mM Tris-HCl, pH 7.5, 1 mM EDTA, 150 mM NaCl). Cells were ruptured by 10 applications of sonication (level 10, 10 s) on ice. After centrifugation at 20,400 × *g* for 10 min at 4°C, and the supernatant was added to 500 µl of glutathione-Sepharose (GE Healthcare) and incubated at 4°C for 1 h. Beads were washed with TES buffer three times. The amount of recombinant proteins on beads was measured by Bradford protein assay (Bio-Rad, Hercules, CA) in the presence of 100 mM reduced glutathione.

In vitro binding assays were modified from Wang and Ferro-Novick (2002). Glutathione-Sepharose beads bound to 100 µg of GST or 200 µg of GST-Ypt3 were preloaded with GDP or GTPγS as follows. The beads were washed with either buffer A (phosphate-buffered saline [PBS], 0.5 mM $MgCl_2$, 1 mM dithiothreitol [DTT], 1 mg/ml bovine serum albumen [BSA], 1 mM phenylmethylsulfonyl fluoride [PMSF], and 1× protease inhibitor cocktail [PIC; Nacalai Tesque, Kyoto, Japan]) or buffer B (PBS, 5 mM $MgCl_2$, 10 mM EDTA, 1 mM DTT, 1 mg/ml BSA, 1 mM PMSF, and 1× PIC) containing 10 µM GTPγS or GDP, respectively. The beads were then incubated with 100 µl of buffer A or buffer B containing 1.5 mM GTPγS or GDP, respectively, at room temperature for 2 h. The wash and incubation steps were repeated once, and then the beads were washed with buffer C (PBS, 10 mM $MgCl_2$, 1 mM DTT, 1 mg/ml BSA, 1 mM PMSF) containing 0.2 mM GTPγS or GDP.

Yeast cells harboring pREP81 (sec2-GFP), pREP81 (spo13-3xGFP), or pREP41 (HA-spo13) were grown in MM+N for 20 h, harvested, and washed with water containing 1 mM PMSF. Next $3.0 \times 10^9$ cells were suspended in 1 ml of lysis buffer (20 mM 4-(2-hydroxyethyl)-1-piperazineethanesulfonic acid, pH 7.2, 100 mM NaCl, 10 mM $MgCl_2$, 1% Triton X-100, 1 mM DTT, 1 mM PMSF, and 1× PIC) before being rapidly frozen in liquid nitrogen. The cells were disrupted by grinding with a pestle and mortar in liquid nitrogen. The lysate was centrifuged at 18,000 × *g* for 15 min, and 50 µl of supernatant was incubated with the prepared beads at 4°C for 2 h in the presence of 0.2 mM GTPγS or GDP. The beads were washed with buffer C containing 10 µM GTPγS or GDP five or more times before analysis.


## ACKNOWLEDGMENTS

We thank R. Sugiura, J. Armstrong, J. Kashiwazaki, I. Mabuchi, and M. Balasubramanian for providing strains, S. Fujita for providing antibody, and C. Shimoda for helpful suggestions. This study was partly supported by a Grant-in-Aid for Scientific Research from the Ministry of Education, Culture, Sports, Science and Technology of Japan (to T.N.). K. I. is the recipient of a Research Fellowship for Young Scientists from the Japan Society for the Promotion of Science.


## REFERENCES


Blümer J, Rey J, Dehmelt L, Mazel T, Wu YW, Bastiaens P, Goody RS, Itzen A (2013). RabGEFs are a major determinant for specific Rab membrane targeting. J Cell Biol 200, 287–300.

Boyd C, Hughes T, Pypaert M, Novick P (2004). Vesicles carry most exocyst subunits to exocytic sites marked by the remaining two subunits, Sec3p and Exo70p. J Cell Biol 167, 889–901.

Cabrera M, Ungermann C (2013). Guanine nucleotide exchange factors (GEFs) have a critical but not exclusive role in organelle localization of Rab GTPases. J Biol Chem 288, 28704–28712.

Cheng H, Sugiura R, Wu W, Fujita M, Lu Y, Sio SO, Kawai R, Takegawa K, Shuntoh H, Kuno T (2002). Role of the Rab GTP-binding protein Ypt3 in the fission yeast exocytic pathway and its connection to calcineurin function. Mol Biol Cell 13, 2963–2976.

Chiba S, Amagai Y, Homma Y, Fukuda M, Mizuno K (2013). NDR2-mediated Rabin8 phosphorylation is crucial for ciliogenesis by switching binding specificity from phosphatidylserine to Sec15. EMBO J 32, 874–885.

Craighead MW, Bowden S, Watson R, Armstrong J (1993). Function of the *ypt2* gene in the exocytic pathway of *Schizosaccharomyces pombe*. Mol Biol Cell 4, 1069–1076.

Das A, Guo W (2011). Rabs and the exocyst in ciliogenesis, tubulogenesis and beyond. Trends Cell Biol 21, 383–386.

Edamatsu M, Toyoshima YY (2003). Fission yeast synaptobrevin is involved in cytokinesis and cell elongation. Biochem Biophys Res Commun 301, 641–645.

Egel R, Egel-Mitani M (1974). Premeiotic DNA synthesis in fission yeast. Exp Cell Res 88, 127–134.

Feng S, Knödler A, Ren J, Zhang J, Zhang X, Hong Y, Huang S, Peranen J, Guo W (2012). A Rab8 guanine nucleotide exchange factor-effector

interaction network regulates primary ciliogenesis. J Biol Chem 287, 15602–15609.
Grosshans BL, Andreeva A, Gangar A, Niessen S, Yates JR 3rd, Brennwald P, Novick P (2006a). The yeast lgl family member Sro7p is an effector of the secretory Rab GTPase Sec4p. J Cell Biol 172, 55–66.
Grosshans BL, Ortiz D, Novick P (2006b). Rabs and their effectors: achieving specificity in membrane traffic. Proc Natl Acad Sci USA 103, 11821–11827.
Guan KL, Dixon JE (1991). Eukaryotic proteins expressed in Escherichia coli: an improved thrombin cleavage and purification procedure of fusion proteins with glutathione S-transferase. Anal Biochem 192, 262–267.
Guo W, Roth D, Walch-Solimena C, Novick P (1999). The exocyst is an effector for Sec4p, targeting secretory vesicles to sites of exocytosis. EMBO J 18, 1071–1080.
Haubruck H, Engelke U, Mertins P, Gallwitz D (1990). Structural and functional analysis of *ypt2*, an essential *ras*-related gene in the fission yeast *Schizosaccharomyces pombe* encoding a Sec4 protein homologue. EMBO J 9, 1957–1962.
Hayles J, Wood V, Jeffery L, Hoe KL, Kim DU, Park HO, Salas-Pino S, Heichinger C, Nurse P (2013). A genome-wide resource of cell cycle and cell shape genes of fission yeast. Open Biol 3, 130053.
Heider MR, Munson M (2012). Exorcising the exocyst complex. Traffic 13, 898–907.
Hergovich A, Stegert MR, Schmitz D, Hemmings BA (2006). NDR kinases regulate essential cell processes from yeast to humans. Nat Rev Mol Cell Biol 7, 253–264.
Hirata A, Shimoda C (1994). Structural modification of spindle pole bodies during meiosis II is essential for the normal formation of ascospores in *Schizosaccharomyces pombe*: ultrastructural analysis of *spo* mutants. Yeast 10, 173–183.
Hirata A, Tanaka K (1982). Nuclear behavior during conjugation and meiosis in the fission yeast *Schizosaccharomyces pombe*. J Gen Appl Microbiol 28, 263–274.
Hutagalung AH, Novick PJ (2011). Role of Rab GTPases in membrane traffic and cell physiology. Physiol Rev 91, 119–149.
Iino Y, Hiramine Y, Yamamoto M (1995). The role of *cdc2* and other genes in meiosis in *Schizosaccharomyces pombe*. Genetics 140, 1235–1245.
Ikemoto S, Nakamura T, Kubo M, Shimoda C (2000). *S. pombe* sporulation-specific coiled-coil protein Spo15p is localized to the spindle pole body and essential for its modification. J Cell Sci 113, 545–554.
Itadani A, Nakamura T, Hirata A, Shimoda C (2010). *Schizosaccharomyces pombe* calmodulin, Cam1, plays a crucial role in sporulation by recruiting and stabilizing the spindle pole body components responsible for assembly of the forespore membrane. Eukaryot Cell 9, 1925–1935.
Kashiwazaki J, Yamasaki Y, Itadani A, Teraguchi E, Maeda Y, Shimoda C, Nakamura T (2011). Endocytosis is essential for dynamic translocation of a syntaxin 1 orthologue during fission yeast meiosis. Mol Biol Cell 22, 3658–3670.
Kita A, Sugiura R, Shoji H, He Y, Deng L, Lu Y, Sio SO, Takegawa K, Sakaue M, Shuntoh H, Kuno T (2004). Loss of Apm1, the micro1 subunit of the clathrin-associated adaptor-protein-1 complex, causes distinct phenotypes and synthetic lethality with calcineurin deletion in fission yeast. Mol Biol Cell 15, 2920–2931.
Knödler A, Feng S, Zhang J, Zhang X, Das A, Peranen J, Guo W (2010). Coordination of Rab8 and Rab11 in primary ciliogenesis. Proc Natl Acad Sci USA 107, 6346–6351.
Ma Y, Kuno T, Kita A, Nabata T, Uno S, Sugiura R (2006). Genetic evidence for phospholipid-mediated regulation of the Rab GDP-dissociation inhibitor in fission yeast. Genetics 174, 1259–1271.
Mata J, Lyne R, Burns G, Bahler J (2002). The transcriptional program of meiosis and sporulation in fission yeast. Nat Genet 32, 143–147.
Matsuyama A, Arai R, Yashiroda Y, Shirai A, Kamata A, Sekido S, Kobayashi Y, Hashimoto A, Hamamoto M, Hiraoka Y, *et al.* (2006). ORFeome cloning and global analysis of protein localization in the fission yeast *Schizosaccharomyces pombe*. Nat Biotechnol 24, 841–847.
Medkova M, France YE, Coleman J, Novick P (2006). The rab exchange factor Sec2p reversibly associates with the exocyst. Mol Biol Cell 17, 2757–2769.
Miyake S, Yamamoto M (1990). Identification of ras-related, *YPT* family genes in *Schizosaccharomyces pombe*. EMBO J 9, 1417–1422.
Mizuno-Yamasaki E, Medkova M, Coleman J, Novick P (2010). Phosphatidylinositol 4-phosphate controls both membrane recruitment and a regulatory switch of the Rab GEF Sec2p. Dev Cell 18, 828–840.
Moreno S, Klar A, Nurse P (1990). Molecular genetic analysis of fission yeast *Schizosaccharomyces pombe*. Methods Enzymol 194, 793–823.
Nachury MV, Loktev AV, Zhang Q, Westlake CJ, Peränen J, Merdes A, Slusarski DC, Scheller RH, Bazan JF, Sheffield VC, *et al.* (2007). A core complex of BBS proteins cooperates with the GTPase Rab8 to promote ciliary membrane biogenesis. Cell 129, 1201–1213.
Nachury MV, Seeley ES, Jin H (2010). Trafficking to the ciliary membrane: how to get across the periciliary diffusion barrier? Annu Rev Cell Dev Biol 26, 59–87.
Nakamura T, Asakawa H, Nakase Y, Kashiwazaki J, Hiraoka Y, Shimoda C (2008). Live observation of forespore membrane formation in fission yeast. Mol Biol Cell 19, 3544–3553.
Nakamura T, Kashiwazaki J, Shimoda C (2005). A fission yeast SNAP-25 homologue, SpSec9, is essential for cytokinesis and sporulation. Cell Struct Funct 30, 15–24.
Nakamura T, Nakamura-Kubo M, Hirata A, Shimoda C (2001). The *Schizosaccharomyces pombe spo3*$^{+}$ gene is required for assembly of the forespore membrane and genetically interacts with *psy1*$^{+}$-encoding syntaxin-like protein. Mol Biol Cell 12, 3955–3972.
Nakamura-Kubo M, Hirata A, Shimoda C, Nakamura T (2011). The fission yeast pleckstrin homology domain protein Spo7 is essential for initiation of forespore membrane assembly and spore morphogenesis. Mol Biol Cell 22, 3442–3455.
Nakamura-Kubo M, Nakamura T, Hirata A, Shimoda C (2003). The fission yeast *spo14*$^{+}$ gene encoding a functional homologue of budding yeast Sec12 is required for the development of forespore membranes. Mol Biol Cell 14, 1109–1124.
Nakase Y, Nakamura T, Hirata A, Routt SM, Skinner HB, Bankaitis VA, Shimoda C (2001). The *Schizosaccharomyces pombe spo20*$^{+}$ gene encoding a homologue of *Saccharomyces cerevisiae* Sec14 plays an important role in forespore membrane formation. Mol Biol Cell 12, 901–917.
Nakase Y, Nakamura T, Okazaki K, Hirata A, Shimoda C (2004). The Sec14 family glycerophospholipid-transfer protein is required for structural integrity of the spindle pole body during meiosis in fission yeast. Genes Cells 9, 1275–1286.
Nakase Y, Nakamura-Kubo M, Ye Y, Hirata A, Shimoda C, Nakamura T (2008). Meiotic spindle pole bodies acquire the ability to assemble the spore plasma membrane by sequential recruitment of sporulation-specific components in fission yeast. Mol Biol Cell 19, 2476–2487.
Neiman AM (1998). Prospore membrane formation defines a developmentally regulated branch of the secretory pathway in yeast. J Cell Biol 140, 29–37.
Neiman AM (2011). Sporulation in the budding yeast *Saccharomyces cerevisiae*. Genetics 189, 737–765.
Ohtaka A, Okuzaki D, Nojima H (2008). Mug27 is a meiosis-specific protein kinase that functions in fission yeast meiosis II and sporulation. J Cell Sci 121, 1547–1558.
Okazaki K, Okazaki N, Kume K, Jinno S, Tanaka K, Okayama H (1990). High-frequency transformation method and library transducing vectors for cloning mammalian cDNAs by trans-complementation of *Schizosaccharomyces pombe*. Nucleic Acids Res 18, 6485–6489.
Ortiz D, Medkova M, Walch-Solimena C, Novick P (2002). Ypt32 recruits the Sec4p guanine nucleotide exchange factor, Sec2p, to secretory vesicles; evidence for a Rab cascade in yeast. J Cell Biol 157, 1005–1015.
Pérez-Hidalgo L, Rozalén AE, Martín-Castellanos C, Moreno S (2008). Slk1 is a meiosis-specific Sid2-related kinase that coordinates meiotic nuclear division with growth of the forespore membrane. J Cell Sci 121, 1383–1392.
Petersen J, Nielsen O, Egel R, Hagan IM (1998). F-actin distribution and function during sexual differentiation in *Schizosaccharomyces pombe*. J Cell Sci 111, 867–876.
Pfeffer SR (2001). Rab GTPases: specifying and deciphering organelle identity and function. Trends Cell Biol 11, 487–491.
Pfeffer SR (2013). Rab GTPase regulation of membrane identity. Curr Opin Cell Biol 25, 414–419.
Segev N (2001). Ypt and Rab GTPases: insight into functions through novel interactions. Curr Opin Cell Biol 13, 500–511.
Shimoda C (2004). Forespore membrane assembly in yeast: coordinating SPBs and membrane trafficking. J Cell Sci 117, 389–396.
Shimoda C, Nakamura T (2004). Control of late meiosis and ascospore formation. In: The Molecular Biology of *Schizosaccharomyces pombe*, ed. R Egel, Berlin: Springer, 311–327.
Stenmark H (2009). Rab GTPases as coordinators of vesicle traffic. Nat Rev Mol Cell Biol 10, 513–525.
Stenmark H, Olkkonen VM (2001). The Rab GTPase family. Genome Biol 2, REVIEWS3007.
Suda Y, Nakano A (2012). The yeast Golgi apparatus. Traffic 13, 505–510.
Takai Y, Sasaki T, Matozaki T (2001). Small GTP-binding proteins. Physiol Rev 81, 153–208.

Takeda T, Imai Y, Yamamoto M (1989). Substitution at position 116 of *Schizosaccharomyces pombe* calmodulin decreases its stability under nitrogen starvation and results in a sporulation-deficient phenotype. Proc Natl Acad Sci USA 86, 9737–9741.

Takeda T, Yamamoto M (1987). Analysis and in vivo disruption of the gene coding for calmodulin in *Schizosaccharomyces pombe*. Proc Natl Acad Sci USA 84, 3580–3584.

Tanaka K, Hirata A (1982). Ascospore development in the fission yeasts *Schizosaccharomyces pombe* and *S. japonicus*. J Cell Sci 56, 263–279.

Tanaka K, Yonekawa T, Kawasaki Y, Kai M, Furuya K, Iwasaki M, Murakami H, Yanagida M, Okayama H (2000). Fission yeast Eso1p is required for establishing sister chromatid cohesion during S phase. Mol Cell Biol 20, 3459–3469.

Toya M, Motegi F, Nakano K, Mabuchi I, Yamamoto M (2001). Identification and functional analysis of the gene for type I myosin in fission yeast. Genes Cells 6, 187–199.

Urbe S, Huber LA, Zerial M, Tooze SA, Parton RG (1993). Rab11, a small GTPase associated with both constitutive and regulated secretory pathways in PC12 cells. FEBS Lett 334, 175–182.

Wang W, Ferro-Novick S (2002). A Ypt32p exchange factor is a putative effector of Ypt1p. Mol Biol Cell 13, 3336–3343.

Wang H, Tang X, Liu J, Trautmann S, Balasundaram D, McCollum D, Balasubramanian MK (2002). The multiprotein exocyst complex is essential for cell separation in *Schizosaccharomyces pombe*. Mol Biol Cell 13, 515–529.

Westlake CJ, Baye LM, Nachury MV, Wright KJ, Ervin KE, Phu L, Chalouni C, Beck JS, Kirkpatrick DS, Slusarski DC, *et al*. (2011). Primary cilia membrane assembly is initiated by Rab11 and transport protein particle II (TRAPPII) complex-dependent trafficking of Rabin8 to the centrosome. Proc Natl Acad Sci USA 108, 2759–2764.

Woods A, Sherwin T, Sasse R, MacRae TH, Baines AJ, Gull K (1989). Definition of individual components within the cytoskeleton of Trypanosoma brucei by a library of monoclonal antibodies. J Cell Sci 93, 491–500.

Yamaoka T, Imada K, Fukunishi K, Yamasaki Y, Shimoda C, Nakamura T (2013). The fission yeast synaptobrevin ortholog Syb1 plays an important role in forespore membrane formation and spore maturation. Eukaryot Cell 12, 1162–1170.

Yang HJ, Neiman AM (2010). A guaninine nucleotide exchange factor is a component of the meiotic spindle pole body in *Schizosaccharomyces pombe*. Mol Biol Cell 21, 1272–1281.

Yoo BY, Calleja GB, Johnson BF (1973). Ultrastructural changes of the fission yeast (*Schizosaccharomyces pombe*) during ascospore formation. Arch Mikrobiol 91, 1–10.

Yoshimura S, Egerer J, Fuchs E, Haas AK, Barr FA (2007). Functional dissection of Rab GTPases involved in primary cilium formation. J Cell Biol 178, 363–369.